Terrain Sensing and Gripping State Determination by a Hand-Eye Camera of a Climbing Robot for Lunar Skylight Exploration

○ Taku Okawara*, Kentaro Uno*, Kazuya Yoshida*

*Space Robotics Labratory, Department of Aerospace Engineering, Tohoku University

Abstract

We have been developing a limed climbing robot that can traverse uneven challenging terrains such as the inside of the Lunar skylight. The robot can climb cliffs by grasping convex terrain (graspable points) with spine grippers. Since the graspable points are given discretely, robust planning requires a wide range and omni-directional 3D terrain mapping. Moreover, even if the robot is controlled to grasp the graspable point, the gripping states determination method in the time has not been established. Therefore, we propose a hand-eye system attached to a camera on the tip of the limb for these problems. In this paper, we introduce the 3D terrain mapping and gripping states determination by the hand-eye system.

月縦孔を探査するクライミングロボットの ハンドアイカメラによる地形認識および把持状態判定

摘要

本研究グループでは，月の縦孔などの凹凸が激しい急傾斜地形を移動探査するための脚型クライミングロボットの研究開発を行っている．同ロボットは，地形内に点在する地形凸部（把持点）に鉤爪型グリッパでしがみ付くことで崖登り移動を可能とする．把持点は離散的に与えられるため，ロバストなプランニングには，広範囲かつ全方向の地図構築が求められる．また，ロボットが把持点を掴むように制御されたとしても，その時の把持状態を判定する手法がまだ確立されていない．そこで，私たちは，脚先にカメラを取り付けるハンドアイシステムでこれらを実現できると考えた．本論文では，ハンドアイシステムによる 3 次元地図構築，把持状態判定を紹介する．

1. Introduction

It is revealed that the lunar has a skylight, a vertical hole, which are thought to be connected to the underground cave.[1] The exploration of this skylight can provide clues to the origin of the Moon. However, it is difficult for conventional wheeled rob-ots to move such a cliff-like terrain. Therefore, our research group has developed a limbed climbing robot. The robot is equipped with a spine gripper at its tip limbs, which are used for grasping the convex point in the terrain. We have clarified the mechanical properties of a spine gripper[3],

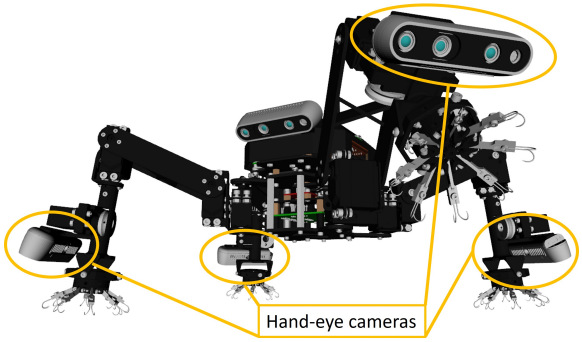

Fig. 1: Limbed climbing robot platform: HubRobo[2] equipped with a hand-eye system.

and proposed an algorithm for detecting convex terrain (graspable points) based on 3D terrain information.[4] We also proposed a non-

periodic gate for the limbed climbing robot by using discrete graspable points.[5)]

We conducted a semi-autonomous experiment with the developed limbed climbing robot based on the 3D terrain map.[2)] This experiment has shown that gripping states determination and a wide range of terrain map in all directions are very important for autonomous limbed climbing robots. To solve these problems, we developed a hand-eye system with a RGB-D camera on each limb of the robot as shown Fig. 1. Therefore, in this paper, we describe building a wide range 3D terrain map and determining gripping states[6)] by using the hand-eye system.

2. A wide range and omni-directional 3D terrain map

In our previous experiments[2)], a camera was only mounted on the robot base and built a terrain map by moving the robot base. Therefore, we think that the robot can efficiently build a wide range terrain map by mounting a camera on the tip of the limb, which has a wide range of motion. Such a camera configuration is called a hand-eye system. Furthermore, by placing the hand-eye camera close to the terrain, it is possible to obtain high-resolution images of the unknown environment, which is very beneficial for planetary exploration.

We use visual SLAM (Simultaneous Localization And Mapping) to build a 3D terrain map in real-time. A map is constructed by overlaying the acquired RGB-D images on it by using an end-effector pose obtained from the forward kinematics of the limb.[7)] A wide range of 3D map in all directions can be constructed by running visual SLAM independently on each hand-eye camera. It is also possible to obtain a detailed shape of terrain by taking a close-up view of it as shown Fig. 2. By building the map of a lunar skylight, the robot will be able to explore it autonomously by detecting the graspable points.[4)5)]

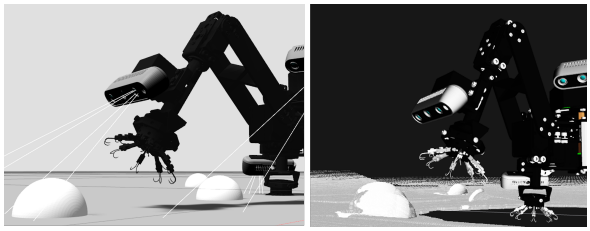

Fig. 2: Obtaining a detailed shape of the terrain(left: prepared terrain, Right: constructed map).

3. Gripping satates determination

In this chapter, we first show the types of gripping states to be determined by our method. Next, we describe in detail the evaluation function and algorithms for determining gripping states.

3.1 Considering gripping states

The unknown environment contains a lot of uncertainties. Thus, even if the terrain map is accurately constructed, it is not always possible to grasp the gripping point properly. Therefore, for the autonomous limbed climbing robot, the robot itself must be able to determine whether the gripping states are proper or not. The proposed method determines four gripping states as shown in Fig. 3.

Case 1 is the state that the gripper is closed. Case 1-1 shows the gripper properly grasps the gripping point (Successful grasping) and Case 1-2 shows the gripper doesn' t properly grasp it (Failed grasping). On the other hand, Case 2 is

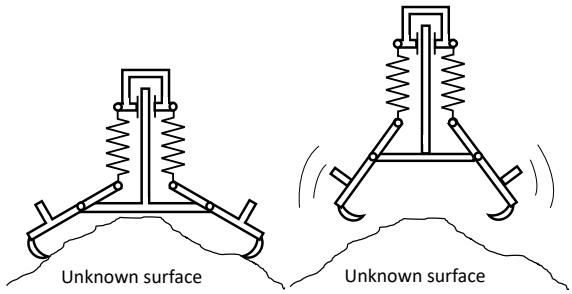

(a) Case 1-1
Successful grasping

(b) Case 1-2
Failed grasping

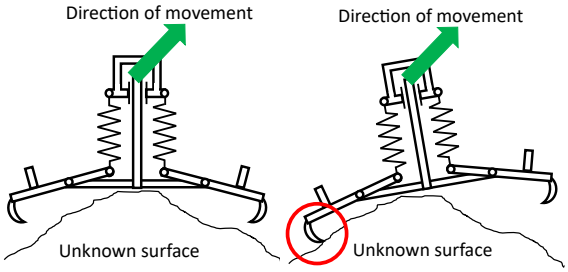

(c) Case 2-1
Successful releasing

(d) Case 2-2
Failed releasing

Fig. 3: Classification of the gripper's states considered in the proposed method.

the state that the gripper is opened. Case 2-1 shows the gripper properly releases the gripping point (Successful releasing) and Case 2-2 shows the gripper doesn't properly release it (Failed releasing). In case of Failed releasing (Fig. 3(d)), The spine of the gripper (circled in red) is caught unintentionally when the robot is controlled to move its leg in the direction of the arrow.

3.2 Evaluation function

When the gripper is hooked on terrain, the limb cannot follow the desired trajectory, regardless of whether the gripper's hooking is desired or not. That is the notable point of our method. In other words, when the limb moves with the gripper hooked, the desired trajectory of the limb and the actual trajectory are different.

We evaluate the difference between the desired and actual limb trajectories by comparing the limb velocity. We calculate the actual end-effector velocity $\boldsymbol{V}_n^{\mathrm{vo}}$ by the time derivative of its position obtained by visual odometry.[8] As shown in Eq. (1), the normalized value of the difference between desired end-effector velocity $\boldsymbol{V}_n^{\mathrm{des}}$ and $\boldsymbol{V}_n^{\mathrm{vo}}$ is used as the evaluation function for determining gripping states. In addition, n represents the number of steps in the time series data and R_n is 0 to 1 because of normalization. R_n represents the degree of coincidence between the two end-effector velocities; if it is 0, these match completely, and if it is 1, these don't match. To improve the robustness against noise, we use a moving weighted average W_n which is a smoothed R_n with the variance of the visual odometry σ_n^2 as weight, as shown in Eq. (2). Therefore, we define W_n as the evaluation function to determine gripping states in the proposed method. Then, N represents the total number of data used to calculate the moving weighted average.

$$R_n = \frac{\left|\boldsymbol{V}_n^{\mathrm{des}} - \boldsymbol{V}_n^{\mathrm{vo}}\right|}{\left|\boldsymbol{V}_n^{\mathrm{des}}\right|} \tag{1}$$

$$W_n = \frac{\sum_{i=0}^{N-1} \sigma_{n-i}^{-2} R_{n-i}}{\sum_{i=0}^{N-1} \sigma_{n-i}^{-2}} \tag{2}$$

3.3 Algorithm of gripping states determination

We describe the algorithm which evaluates W_n and determines Successful grasping and Failed grasping when the gripper is closed, and Successful releasing and Failed releasing when

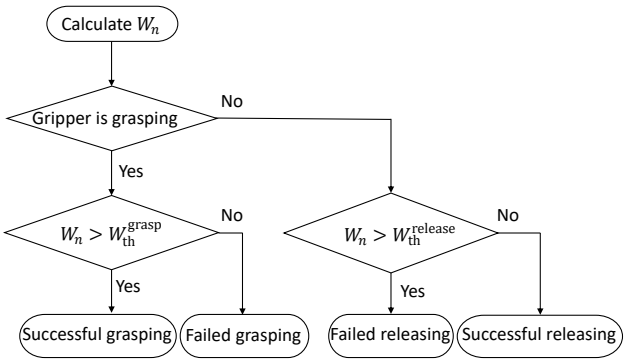

Fig. 4: Flow chart for the proposed method to determine the gripper's state.

the gripper is opened. When a grasping command is given to the gripper, if W_n is close to 0, the spine is hooking, and if W_n is close to 1, it is not hooking. By focusing on such a dramatic change of W_n, our gripping states determination method is done.

As shown in Fig. 4, we can determine the gripping states by defining the threshold for W_n according to the opening and closing of the gripper. The threshold when the gripper is closed is $W_{\text{th}}^{\text{grasp}}$ and the gripper is open is $W_{\text{th}}^{\text{release}}$. When the gripper is closed (Case 1), if W_n is greater than $W_{\text{th}}^{\text{grasp}}$, it is determined as Successful grasping. On the other hand, if W_n is less than $W_{\text{th}}^{\text{grasp}}$, it is determined as Failed grasping. We have summarized Case 1, and the same applies to Case 2. Therefore, $W_{\text{th}}^{\text{grasp}}$ and $W_{\text{th}}^{\text{release}}$ satisfy Eq. (3) and Eq. (4), respectively.

$$W_{n,\text{failed}}^{\text{grasp}} < W_{\text{th}}^{\text{grasp}} < W_{n,\text{successful}}^{\text{grasp}} \tag{3}$$

$$W_{n,\text{successful}}^{\text{release}} < W_{\text{th}}^{\text{release}} < W_{n,\text{failed}}^{\text{release}} \tag{4}$$

4. Validation

In this chapter, we describe the verification of the terrain mapping by simulation and gripping states determination by experiment.

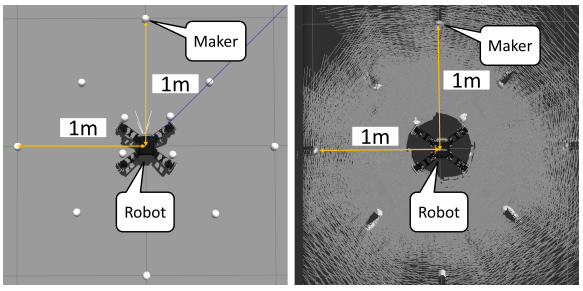

Fig. 5: Mapping simulation(left: prepared environment, Right: constructed map).

4.1 Simulation condition about terrain mapping

Visual SLAM with a hand-eye system consisting of four cameras is verified by gazebo and ROS (Robot Operation System). By inputting the acquired images into visual SLAM, a 3D terrain map is constructed on RViz, ROS visualization tool. We use the virtual RGB-D camera by using realsense_gazebo_plugin.

4.2 Simulation result about terrain mapping

The constructed map is shown in Fig. 5 for qualitative evaluation. We can confirm that a wide range of 3D terrain map in all directions has been constructed successfully. Next, both gazebo and RViz have a 1m grid drawn on them, and the position of the white target on the map is almost identical to the one on the gazebo.

4.3 Experimental condition about gripping states determination

The experimental environment is shown in Fig. 6. By mounting a hand-eye camera to the left front limb, we experimented five times in each Case according to the following procedure.

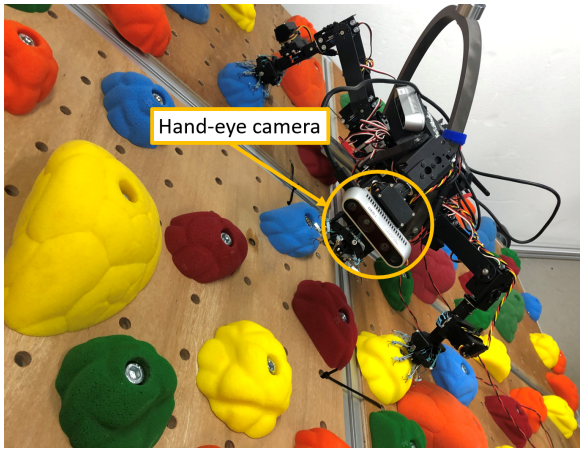

Fig. 6: Experimental condition for gripping states determination.

1) Send a command to the left front end-effector to move in a straight line for 5 seconds.
2) Calculate the end-effector position based on forward kinematics and visual odometry respectively.
3) Calculate the end-effector velocities $\boldsymbol{V}_n^{\mathrm{vo}}$ and $\boldsymbol{V}_n^{\mathrm{des}}$ by differentiating its position.
4) Calculate W_n.

4.4 Experimental result about gripping states determination

The time histories of the number n for W_n in Case 1-1 and Case 1-2, Case 2-1 and Case 2-2 are shown in Fig. 7 and Fig. 8, respectively. From Fig. 7 and Fig. 8,we find the minimum values of W_n from Case 1-1 and Case 2-2, $W_{n,\mathrm{successful}}^{\mathrm{grasp}}$ and $W_{n,\mathrm{failed}}^{\mathrm{release}}$. Similarly, we find the maximum values of W_n from Case 1-2 and Case 2-1, $W_{n,\mathrm{failed}}^{\mathrm{grasp}}$ and $W_{n,\mathrm{successful}}^{\mathrm{release}}$.From Fig. 7, we obtain $W_{n,\mathrm{successful}}^{\mathrm{grasp}} = 0.89$, $W_{n,\mathrm{failed}}^{\mathrm{grasp}} = 0.58$. From Fig. 8, we obtain have $W_{n,\mathrm{successful}}^{\mathrm{release}} = 0.76$ and $W_{n,\mathrm{failed}}^{\mathrm{release}} = 0.91$. Therefore, we verify that it is possible to define the threshold for determining gripping states properly. By applying this threshold to the algorithm of Fig. 4, the limbed climbing robot can determine gripping states in real-time.

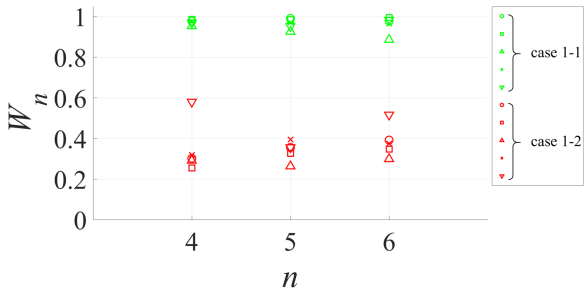

Fig. 7: Experimental results for Case 1-1 and Case 1-2.

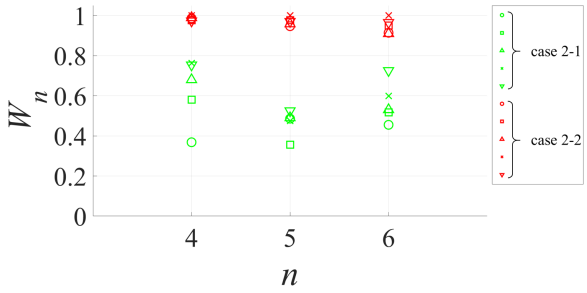

Fig. 8: Experimental results for Case 2-1 and Case 2-2.

5. Conclusion

In this paper, we introduced 3D terrain mapping using the hand-eye system and proposed gripping states determination method for the limbed climbing robot. We can construct a wide range of 3D terrain map by using visual SLAM with four camera images as input. By setting the threshold appropriately, it is possible to determine Successful grasping and Failed grasping when the gripper is closed, and Successful releasing and Failed releasing when the gripper is opened. In the future, we will consider the robot's operation to return from an improper gripping state to proper it.

Acknowledgement

This work is supported by JSPS KAKENHI Grant Number 19J20685.

Reference

1) T. Kaku, J. Haruyama, W. Miyake, A. Kumamoto, K. Ishiyama, T. Nishibori, K. Yamamoto, S. T. Crites, T. Michikami, Y. Yokota, *et al.*, "Detection of intact lava tubes at Marius Hills on the Moon by SELENE (Kaguya) Lunar Radar Sounder," *Geophysical Research Letters*, vol. 44, no. 20, pp. 10–155, 2017.

2) K. Uno, N. Takada, T. Okawara, K. Haji, A. Candalot, W. F. Ribeiro, K. Nagaoka, and K. Yoshida, "Hubrobo: a lightweight multi-limbed climbing robot for exploration in challenging terrain," in *2020 IEEE-RAS 20th International Conference on Humanoid Robots (Humanoids)*, 2021, pp. 209–215.

3) K. Nagaoka, H. Minote, K. Maruya, Y. Shirai, K. Yoshida, T. Hakamada, H. Sawada, and T. Kubota, "Passive Spine Gripper for Free-Climbing Robot in Extreme Terrain," *IEEE Robotics and Automation Letters*, vol. 3, no. 3, pp. 1765–1770, 2018.

4) K. Haji, K. Uno, K. Nagaoka, and K. Yoshida, "Gripping Target Detection in Terrain Based on Geometrical Configuration of a Gripper for Free-Climbing Robots (in Japanese)," in *Proceedings of JSME annual Conference on Robotics and Mechatronics (Robomech)*, no. 2P1-B06, 2020.

5) K. Uno, Y. Koizumi, K. Haji, M. Keiff, S. Harms, W. F. Ribeiro, W. Jones, K. Nagaoka, and K. Yoshida, "Non-Periodic Gait Planning Based on Salient Region Detection for a Planetary Cave Exploration Robot," no. 5027, 2020.

6) T. Okawara, K. Uno, N. Takada, and K. Yoshida, "Gripping State Determination Method Using a Hand-Eye Camera for a Legged Climbing Robot (in Japanese)," in *Proceedings of the 331st Workshop on the Society of Instrument and Control Engineers at Tohoku Chapter*, no. 331-2, 2021.

7) M. Labbé and F. Michaud, "RTAB-Map as an open-source lidar and visual simultaneous localization and mapping library for large-scale and long-term online operation," *Journal of Field Robotics*, vol. 36, no. 2, pp. 416–446, 2019.

8) D. Scaramuzza and F. Fraundorfer, "Visual odometry [tutorial]," *IEEE Robotics and Automation Magazine*, vol. 18, no. 4, pp. 80–92, 2011.